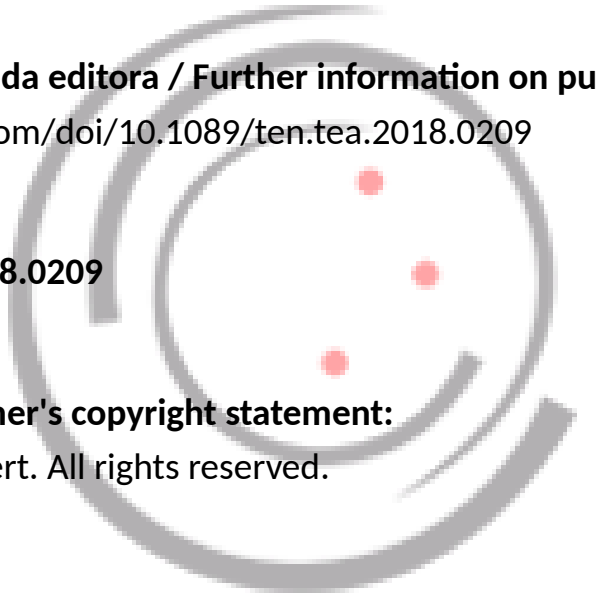

TISSUE ENGINEERING: Part A
Volume 25, Numbers 15 and 16, 2019

DOI: 10.1089/ten.tea.2018.0209

termis
Tissue Engineering
& Regenerative Medicine
International Society

ORIGINAL ARTICLE

Periodontal Tissue Regeneration Using Brain-Derived Neurotrophic Factor Delivered by Collagen Sponge

Ilana Ramalho, DDS, MSc,[1,2] Edmara Bergamo, DDS, MSc,[2,3] Adolfo Lopes, DDS,[1,2]
Camille Medina-Cintrón, DMD, MS,[4] Rodrigo Neiva, DDS, MSc,[4]
Lukasz Witek, MSc, PhD,[2] and Paulo Coelho, DDS, PhD[2]

Aim: To evaluate the influence of brain-derived neurotrophic factor (BDNF) in combination with collagen sponges on periodontal tissue regeneration.
Methods: Unilateral, ''box-type'' (4×5 mm), one-wall intrabony defects were surgically created at posterior mandibular teeth in 14 Beagle dogs. Animals received all experimental groups, and the defects were randomly treated as follows: Emdogain® (positive control) [EMD]; HeliPlug®+BDNF [H/B]; RCP®+BDNF [R/B]; negative control [Control]; TeruPlug®+BDNF [Tp/B]; and TeruPlug®+BDNF2 [Ts/B]. Periodontal wound healing was observed every 2 weeks by computed tomography. The animals were euthanized at 8 weeks postsurgery for microcomputed tomography and histomorphometric evaluation.
Results: All groups presented ~ 1 mm apical epithelial attachment relative to cementoenamel junction. Although linear measurements did not demonstrate significant differences between groups for cementum and periodontal ligament regeneration, semiquantitative analysis depicted higher percentage of samples with mineralized cementum and functional PDL for Ts/B, R/B, and H/B groups relative to EMD and Control ($p < 0.046$). Irrespective of quantification method (2D or 3D), Ts/B, Control, Tp/B, and H/B groups presented the highest mean percentage of new bone (not significantly different) followed by R/B and EMD groups.
Conclusion: While no significant differences were detected in quantitative analyses, Ts/B combination results in significantly more samples with full periodontal tissue regeneration relative to control groups.

Keywords: BDNF, brain-derived neurotrophic factor, periodontal regeneration, emdogain, collagen sponge

Impact Statement

The various roles played by brain-derived neurotrophic factor (BDNF) in a multitude of tissues and at different scenarios have rendered BDNF a favorable candidate for improving tissue regeneration. Although the tested formulations of BDNF quantitatively regenerate tissue to a level similar to control groups, it resulted in significantly more instances of full regeneration.

Introduction

Periodontitis is a chronic inflammatory disorder in response to infectious agents, which has been estimated to severely affect approximately 15% of the worldwide adult population.[1,2] Such a disease is characterized by loss of connective tissue attachment and destruction of the supporting bone that in the worst-case scenario may result in tooth loss.[3] Conventional treatment methods for periodontitis include scaling and root planing or open flap debridement, which have been demonstrating consistent results concerning the prevention of the disease recurrence.[4] Nonetheless, the ultimate goal and certainly the most difficult challenge of periodontal treatment is to regenerate the once lost tissue as a consequence of periodontitis.[5,6]

Typically, periodontal tissue consists of heterogeneous cell populations that are arranged over time to form the complex structure necessary for supporting the tooth.[7] Therefore, a successful regenerative therapy requires the reconstruction of a functional periodontium, which is structured

[1]Department of Prosthodontics and Periodontology, Bauru School of Dentistry, University of Sao Paulo, Bauru, Brazil.
[2]Department of Biomaterials and Biomimetics, New York University College of Dentistry, New York, New York.
[3]Department of Prosthodontics and Periodontology, Piracicaba Dental School, University of Campinas, Piracicaba, Brazil.
[4]Department of Periodontology, College of Dentistry, University of Florida, Gainesville, Florida.
This work was performed at the Department of Biomaterials and Biomimetics, New York University College of Dentistry, New York, New York.

with a newly formed cementum, regenerated alveolar bone, and periodontal ligament (PDL) encompassing functionally oriented connective tissue fibers inserted into the hard tissues.[8] The early stage of periodontal tissue regeneration comprises the proliferation and the migration of PDL cells along the tooth root, differentiating into cementoblasts or osteoblasts.[9] Accordingly, treatment modalities such as the application of enamel matrix protein derivatives (EMD) and/or the delivery of growth factors that directly modulate cell proliferation and differentiation rates have been explored.[5,10–15]

Brain-derived neurotrophic factor (BDNF), a member of the neurotrophin family, has been shown to play an essential role not only in the survival and differentiation of central and peripheral neurons but also in various types of non-neural cells such as PDL cells, cementoblasts, and endothelial cells. BDNF modulates cellular function by binding to appropriate high-affinity receptors, such as tropomyosin receptor kinase B (TrkB).[6,16–18] It has been demonstrated that neurotrophins are associated with the development of human and mouse teeth since it is expressed in the tooth germ.[19,20] It is therefore hypothesized that mimicking the biological process may lead to the generation of a successful multiple tissue regenerative therapy.[18]

To date, sparse information is available concerning the actual role of BDNF on the cementum and PDL cells, and more studies are strongly warranted to elucidate the molecular mechanisms underlying BDNF action that can help to design treatment strategies. According to previous studies, the mechanism in which BDNF can modulate periodontal tissue regeneration rate is speculated to be associated with an elevated synthesis of bone (cementum)-related proteins such as alkaline phosphatase, osteopontin, bone morphogenetic protein-2, and type I collagen in PDL cells and cementoblasts, known to result in the proliferation and differentiation of PDL cells.[6,18] These studies also suggest that BDNF stimulates angiogenesis by regulating endothelial cell function, as well as acts on the upregulation of such cellular functions by binding to TrkB receptors.

Accordingly, the various roles played by BDNF in a multitude of tissues and at different clinical scenarios have rendered BDNF a favorable candidate for improving tissue regeneration to restore form and function.[5,6,10,18–22]

Furthermore, an ideal release of a tissue regenerating factor involves the selection of an appropriate carrier whose requirements aside from biocompatibility include structural integrity, defined release kinetics, and uneventful biodegradation that matches the rate of new tissue formation.[12] There currently is a trend to use naturally-derived materials employing the principles of tissue engineering, such as collagen-based matrices/scaffolds.[23,24]

Absorbable collagen sponges are considered the benchmark due to their biological properties, such as outstanding hemostatic, chemotactic, and cell adhesive characteristics that stimulate cells to infiltrate, adhere, and synthesize new tissue.[25–29] Previous reports have demonstrated the ability of collagen sponges to adsorb growth factors and remarkably enhance periodontal tissue regeneration.[12,13,15] Nonetheless, at present, the potential synergistic effect of the BDNF locally delivered by collagen sponges on accelerating periodontal tissue regeneration has not been addressed yet. Therefore, the aim of the current study was to evaluate the influence of BDNF in combination with collagen sponges on periodontal tissue regeneration compared to an enamel matrix derivative standard product (EMD - Emdogain®) and a negative control group (Control).

Materials and Methods

Preclinical in vivo *model*

Following approval by the BWEF Institutional Animal Care and Use Committee (IACUC), NJ, 14 healthy, female beagle dogs (12 months of age) were acquired and acclimatized to the animal facility for 7 days before surgical intervention.

All surgeries were performed under aseptic conditions in a designated animal operation suite under general anesthesia. As per the standard procedure, on the day of the surgery, the animals were weighed and then premedicated with an intramuscular administration of atropine sulfate (0.044 mg/kg) and xylazine chlorate (8 mg/kg). Then, general anesthesia was induced following an intramuscular injection of ketamine chlorate (12 mg/kg) (Ketalar Vet®; Pfizer AB, Sollentuna, Sweden) and midazolam (0.3 mg/kg, Dormicum®; Roche, Basel, Switzerland). The animals were monitored until unconscious, intubated, and general anesthesia was achieved and maintained through the administration of 2.5% isoflurane.

The first surgical procedure comprised the extraction of the mandibular first molar and third premolar teeth in the right and left quadrants. After healing, experimental surgeries were performed through buccal and lingual mucoperiosteal flap elevation to create three bilateral, ''box-type'' (4×5 mm), one-wall intrabony defects at the mesial aspect of the second mandibular molar and distal aspect of second and fourth mandibular premolar teeth using a cylindrical bur. A reference notch was placed with a round bur into the root surface at the level of the alveolar crest to aid histologic identification of new periodontal tissues. Once the defect was created, curettes and rotary instrumentation were used to remove the PDL and root cementum.

All animals received all experimental groups, which were randomly assigned for each defect site resulting in a balanced study design. For all but the defects receiving Emdogain (Straumann, Basel, Switzerland) the denuded root surface was cleaned with 14–18% EDTA (pH 7.0). The sites receiving Emdogain were pretreated with PrefGel® (Straumann, Basel, Switzerland) according to manufacturer's instructions. The preconditioning was followed by rinsing with sterile saline for all defects, avoiding contamination of the root surface with saliva or blood after last rinse. After the preparation of the surgical site, the defects were treated as follows:

- EMD: Emdogain (Straumann, Basel, Switzerland).
- H/B: Collagen, HeliPlug® (Integra Miltex, York, PA) + BDNF (Sigma-Aldrich®, St. Louis, MO).
- R/B: Collagen, RCP® (Resorbable Collagen Plug, ACE Surgical Supply Co., Inc., Brockton, MA) + BDNF (Sigma-Aldrich).
- Control: Negative control.
- Tp/B: Collagen, TeruPlug® (Terumo Corp., Tokyo, Japan), + BDNF (Sigma-Aldrich).
- Ts/B: Collagen, TeruPlug (Terumo Corp.), + BDNF2 (Sumitomo Dainippon Pharma Co., Ltd., Tokyo, Japan).[21,30]

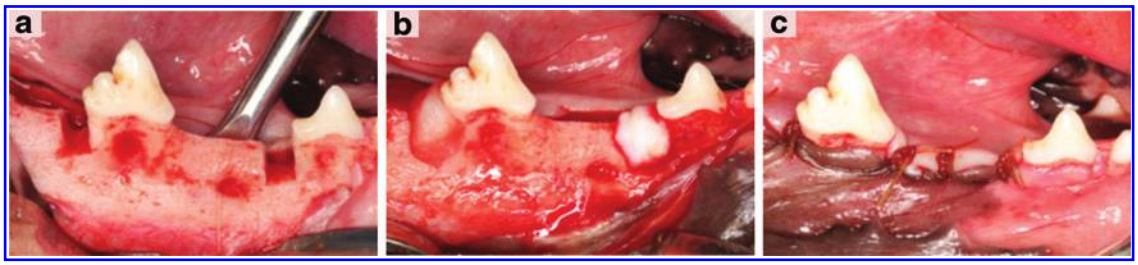

FIG. 1. **(a)** Surgical creation of one-wall intrabony defects **(b)** defect filled to the level of the alveolar crest with the different materials covering the denuded root surface and **(c)** mucogingival flaps sutured with a nonabsorbable suture. Color images are available online.

Before application into the prepared defects the collagen sponges were presoaked with 100 µL of a BDNF solution (500 µg/mL, reconstituted in phosphate-buffered saline). The defect sites were filled to the level of the alveolar crest with the different materials covering the denuded root surface, except the S group which remained empty and served as a negative control. In all cases, the mucogingival flaps were sutured using a nonabsorbable suture (Fig. 1).

After surgery, animals were subjected to a soft diet to prevent incision line opening. Postoperative medication included antibiotics (penicillin, 20,000 UI/kg) and anti-inflammatory (ketoprophen, 1 mL/5 kg) for a period of 48 h. Euthanasia was performed 8 weeks after the experimental surgical procedure by anesthesia overdose.

CT and µCT 3D reconstructions

The evaluation of new bone within defects was performed by Computed tomography (CT) (GE NXI Pro; GE Medical Systems, Madison, WI) and microcomputed tomography (µCT) (µCT 40; Scanco Medical, Basserdorf, Switzerland).

CT scans were performed at baseline (2 days after experimental surgery) and at 2, 4, 6, and 8 weeks post-intervention. Three-dimensional rendering of the image sets was performed using a standard ''bone mask'' (bluescale–baseline; grayscale–subsequent time points) in Amira software (Amira 6.3.0; FEI Company, Berlin, Germany) (Fig. 2a, b). The same software was used to realign the mandibles along the physiological axes, and anatomic landmarks were used to ensure that the scans at different time points were all aligned in an identical manner (Fig. 2b). The region of interest (ROI) was defined by a box-shaped contour of the intact bone from the baseline scan and was fixed within each defect for evaluation at 2, 4, 6, and 8 weeks (Fig. 2c, d). A uniform threshold for bone was determined across all samples using the Otsu algorithm and the bone defect ROIs. Bone volume (BV) to total volume (TV) ratio was determined on the CT images for all time points.

For the purpose of obtaining higher resolution data regarding bone healing in this model, µCT imaging was also used to analyze BV/TV ratio in the defect space. The X-ray energy level used was 70 kVp and the current level 114 µA. All data were exported in a DICOM format and imported into Amira software for 3D reconstruction and quantification. The same protocol of image superimposition was used to realign the mandible µCT scans to the baseline CT data (Fig. 2e–g). The percent bone formation was calculated (Fig. 2h).

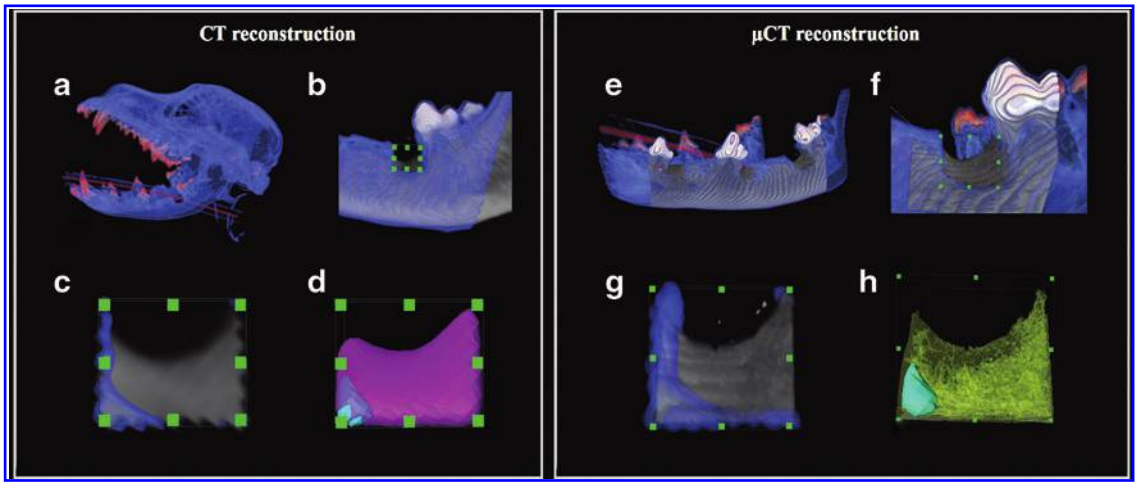

FIG. 2. Three-dimensional CT and µCT reconstructions. **(a)** Three-dimensional rendering of baseline (*bluescale*) and **(b)** 8 weeks (*grayscale*) CT image sets. **(b, c)** ROI defined by a *box-shaped* contour involving full defect volume (standardized through different time point superimpositions). **(d)** Three-dimensional reconstruction of baseline (*blue*) and 8 week (*pink*) superimposition. **(e)** Superimposition of baseline CT (*bluescale*) and µCT (*grayscale*) reconstructions. **(f, g)** ROI defined by a box-shaped contour involving full defect volume (standardized through different time point superimpositions). **(h)** Three-dimensional reconstruction of baseline (*blue*) and 8 week (*yellow*) superimposition. ROI, region of interest. Color images are available online.

Histomorphometry

Following euthanasia, the specimens were fixed in 10% buffered formalin for 48 h, and following μCT the mandibles were reduced to blocks containing one defect each. The blocks were gradually dehydrated in a series of alcohol solutions ranging from 70% to 100% ethanol. Following dehydration, the samples were embedded in a methacrylate-based resin (Technovit 9100, Heraeus Kulzer GmbH, Wehrheim, Germany) according to the manufacturer's instructions. The blocks were then cut into slices (~300 μm thick) centering the tooth according to its long axis with a precision diamond saw (IsoMet 2000; Buehler Ltd., Lake Bluff, IL) and glued to acrylic plates with an acrylate-based cement (Technovit 7210 VLC; Heraeus Kulzer GmbH, Wehrheim, Germany), and a 24-h setting time was allowed before grinding and polishing. The sections were vertically generated in a mesial distal direction within the defect. The sections were then reduced to a final thickness of ~80 μm by means of a series of silicon carbide (SiC) abrasive papers (400, 600, 800, 1200, and 2500; Buehler Ltd.) in a grinding/polishing machine (MetaServ 3000; Buehler Ltd.) under water irrigation. Subsequently, the samples were stained with Stevenel's Blue and Van Gieson's Picro Fuchsin (SVG) and digitally scanned using an automated slide scanning system and in specialized computer software (Aperio Technologies, Vista, CA).

Semiquantitative analysis. The defect margins of each histologic representative section were delimitated involving the area of the denuded root and their respective adjacent structures (Fig. 3a). Then, the defect area of each micrograph was semiquantitatively classified according to periodontal tissue regeneration as no epithelial migration, epithelial apical migration, no cementum, mineralized cementum, mineralized cementum and cementoid tissue, non- and full periodontal ligament, and nonfunctional and functional PDL, parameters detailed in Table 1. In addition, areas not surgically treated presenting typical anatomic features of periodontal tissue were used as reference for semiquantitative assessment (Fig. 3b, c).

Quantitative analysis. After delimitation of the defect margins, percent bone formation within defect (from bone height before defect creation) was quantified by means of computer software (ImageJ, NIH, Bethesda). Quantitative linear measurements of epithelial apical migration, no cementum, mineralized cementum, mineralized cementum and cementoid tissue, non- and full periodontal ligament, and non- and functional PDL were performed along the tooth. Following linear measurement in mm, the % epithelial apical migration, % mineralized cementum, % mineralized cementum and cementoid, % PDL, and % functional PDL were calculated as a function of the length where full PDL regeneration was possible (between tooth and regenerated bone) (Fig. 3d).

Statistical analyses

Statistical evaluation of percent bone formation within defect through CT, μCT, 2D quantification, and histomorphometric linear measurements was performed using linear mixed model analysis of variance and least significant difference *post hoc* analyses with fixed factors of time and group for CT (2-, 4-, 6-, and 8-week *in vivo*) and group for μCT, 2D quantification, and histomorphometric linear measurements.

For semiquantitative analysis and cross tabulation, samples were classified as full regeneration (samples with NEM; 100% tissue of interest regeneration for all other outcomes evaluated) and nonfull regeneration (samples with EM; and no or partial regeneration of tissue of interest). Cross tabulated nonfull and full regeneration histologic data were assessed by generalized estimating equations (GEEs) with a logistic link to estimate effects of group on each tissue outcome. This approach is conceptually similar to logistic regression, but optimized for nested within subject observations. In all analyses, *post hoc* comparisons were based on estimated confidence limits using the pooled estimate of the standard error for the mixed model analysis of variance and Wald estimates for the GEE model.

All statistical analyses of data were performed using IBM SPSS (v23; IBM Corp., Armonk, NY), and the data are presented as a function of mean and 95% confidence interval.

Results

No postoperative complications were detected in any of the animals regarding infection and/or other clinical concern. In

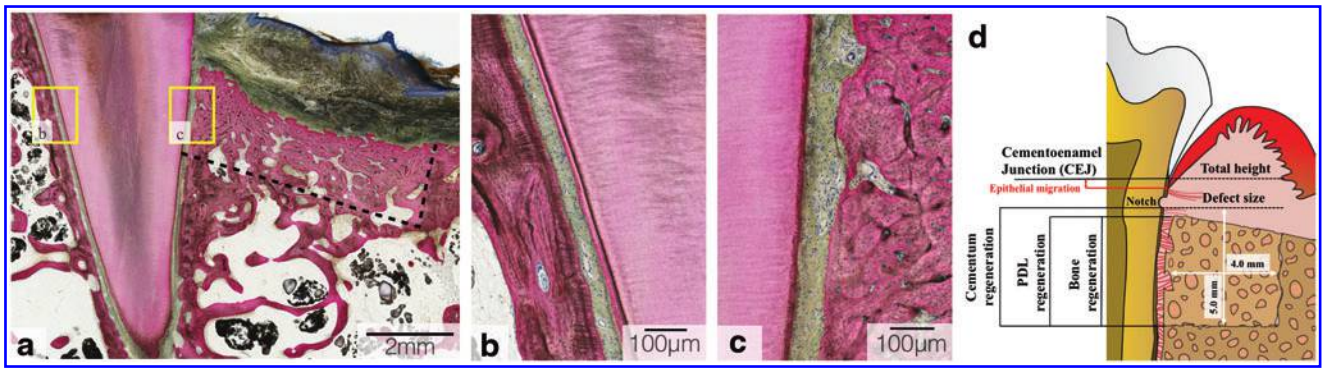

FIG. 3. **(a)** A descriptive histologic section delimiting defect margins (marked in *black*). **(b)** Typical anatomic features of hard (alveolar bone, cementum, and root dentin) and soft tissues (periodontal ligament). **(c)** Morphological features of regenerated mineralized cementum, PDL, and new bone. **(d)** Schematic diagram of the landmarks used in the quantitative analysis. PDL, periodontal ligament. Color images are available online.

Table 1. Typical Anatomic Features Adopted for Qualitative Analysis of Epithelial Tissue Attachment, Cementum, and Periodontal Ligament Regeneration

Parameter	*Data collection*	*Meaning*
No epithelial apical migration (NEM)	Samples with epithelial attachment at the level of cementoenamel junction	Quantity of samples with no epithelial tissue apical migration
Epithelial apical migration (EM)	Samples with apical migration of epithelial attachment relative to cementoenamel junction	Quantity of samples with epithelial tissue apical migration
No Cementum (NC)	Samples with no defect dentin coverage with mineralized cementum	Quantity of samples with no mineralized cementum
Mineralized Cementum (MC)	Samples with defect dentin full coverage with newly formed mineralized cementum (cellular, acellular, and mixed cellular + acellular)	Quantity of samples with mineralized cementum only, that is, without portions of cementoid tissue
Mineralized Cementum + Cementoid Tissue (CCT)	Samples with defect dentin coverage with newly mineralized cementum and nonmineralized cementoid tissue	Quantity of samples with both mineralized cementum and cementoid tissue
Nonfull Periodontal Ligament (NFPDL)	Samples with no and partial PDL regeneration	Quantity of samples with no or partial PDL. The latter is represented by partial fibrous content bridging new bone and mineralized cementum and/or cementoid tissue
Full Periodontal Ligament (FPDL)	Samples with full fibrous content bridging new bone and mineralized cementum and/or cementoid tissue	Quantity of samples with full fibrous content bridging new bone and mineralized cementum and/or cementoid tissue
Nonfunctional PDL (NFcPDL)	Samples with full fibrous content bridging new bone and mineralized cementum and cementoid tissue	Quantity of samples with full fibrous content bridging new bone and mineralized cementum and cementoid tissue, that is, without portions of pure mineralized cementum.
Functional PDL (FcPDL)	Samples with full fibrous content bridging new bone and mineralized cementum	Quantity of samples with full fibrous content bridging new bone and mineralized cementum, that is, without portions of cementoid tissue

addition, following euthanasia, sharp dissection of the mandible defects did not reveal any sign of inflammation and/or infection.

Epithelial tissue apical migration

Representative histologic sections of samples with and without EM are presented in Figure 4a, b. GEE analysis depicted that the Control and Ts/B groups presented higher percentage of samples with epithelium apical attachment (90%, CI:53–99%) (both significantly different from H/B group, 50% CI:24–76%), ($p = 0.009$) (Tables 2 and 3). In contrast, the percentage of epithelial tissue apical attachment as a function of defect depth (quantitative data) demonstrated no significant difference between groups ($p = 0.767$). In fact, all groups presented approximately 1 mm apical epithelial attachment relative to cementoenamel junction (CEJ), which represents approximately 15% of the distance between CEJ and the defect depth (Fig. 5).

Cementum regeneration

Histologic representative images depicted a significant amount of new cementum formed along the notch and the root surface for all groups. In addition, higher magnification micrographic observations demonstrated the different stages of tissue regeneration due to the presence of cementoid tissue over dentin and mineralized cementum regeneration (that comprised cellular, acellular, and mixed cellular + acellular cementum). The images showed the presence of cementoblasts along with an unmineralized precementum on the root surface (cementoid tissue) and the morphologic similarity between regenerated mineralized cementum and typical cementum (Fig. 4c–h).

Cross tabulated data and GEE analysis showed that the percentage of samples presenting 100% mineralized cementum regeneration between the tooth and regenerated bone for Ts/B (27%, CI:9–59%), H/B (25%, CI:8–55%), and R/B (25%, CI:8–55%) groups was significantly higher than EMD and Control ($p < 0.042$) groups, which did not present any sample with full mineralized cementum regeneration (0%, CI:0–0%) (Tables 2 and 3). Ts/B (73%, CI:41–91%) and EMD (78%, CI:42–94%) groups presented high percentage of samples with mineralized cementum + cementoid tissue covering 100% of the root surface within bone walls. The latter was statistically significantly different from Control group (40%, CI:42–94%) ($p = 0.022$) (Tables 2 and 3).

Considering linear measurements, no significant difference was noted between groups regarding the percentage of mineralized cementum within regenerated bone and tooth ($p > 0.90$) (mean percentage ranging from 44% to 59%) (Fig. 6a). Percent of cementum + cementoid tissue

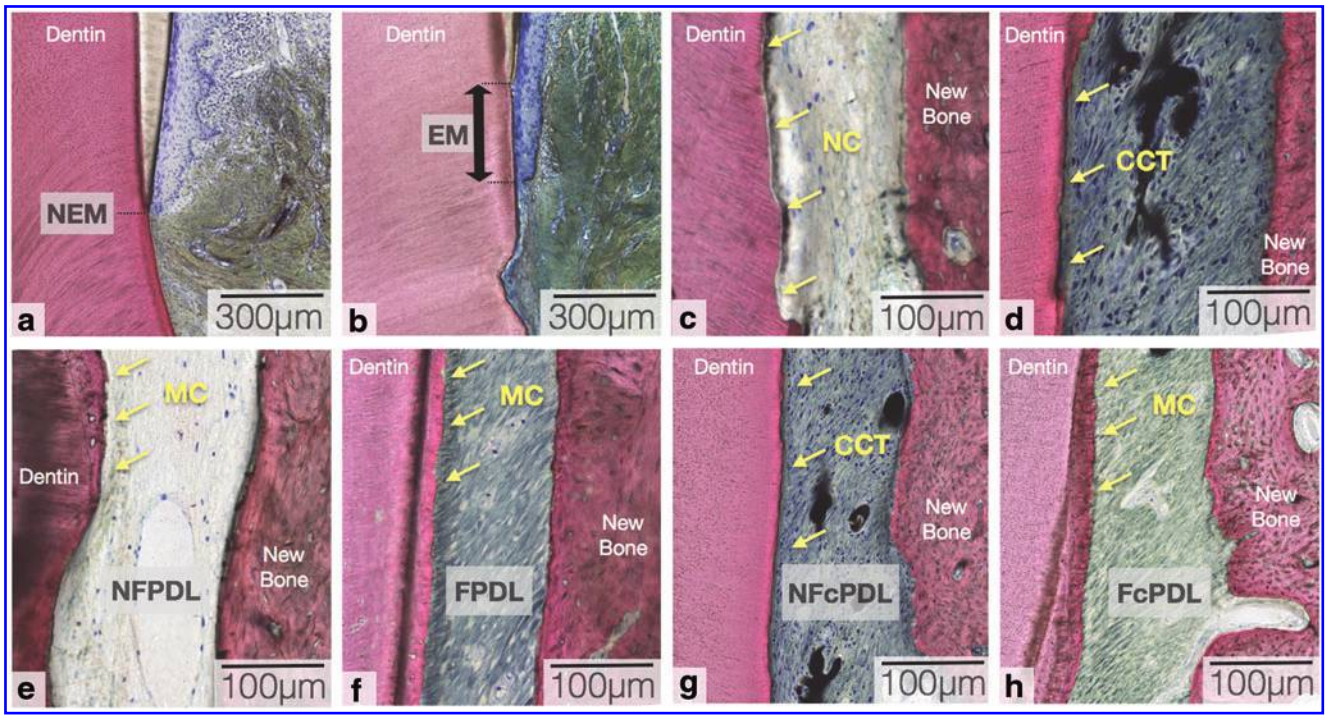

FIG. 4. Histomorphologic features of **(a)** no epithelial apical migration (NEM), **(b)** epithelial apical migration (EM), **(c)** no cementum (NC), **(d)** cementum + cementoid tissue (CCT), **(e)** mineralized cementum (MC) and nonfull PDL (NFPDL), **(f)** mineralized cementum (MC) and full PDL (FPDL), **(g)** nonfunctional PDL (NFcPDL), and **(h)** mineralized cementum (MC) and functional PDL (FcPDL). *Arrows* indicate areas of interest. Color images are available online.

demonstrated significantly higher values for Ts/B group (96%, CI: ±11.4%) relative to H/B (80%, CI: ±10.9%) ($p = 0.044$). All other group comparisons were statistically homogeneous, ($p > 0.05$), with mean percentage of cementum + cementoid tissue regeneration up to 87% (Fig. 6b).

PDL regeneration

Representative histologic sections depicting non-full PDL regeneration, full PDL regeneration, nonfunctional PDL regeneration, and functional PDL regeneration are presented in Figure 4e–h. Full PDL regeneration only occurred when mineralized cementum and/or cementoid tissue fully covered instrumented dentin in which the new perpendicularly or obliquely oriented PDL fibers bridged the gap between the formed cementum and bone (Fig. 4f, g). Functional PDL was characterized by root coverage with mineralized cementum and regenerated bone bridged with the newly formed fibers (Fig. 4h).

Cross tabulated data and GEE analysis of PDL regeneration demonstrated higher percentage of samples with full PDL regeneration between tooth and regenerated bone for Ts/B (62%, CI:34–86%) and EMD (44%, CI:18–75%) groups compared to Control (10%, CI:1–47%) and H/B (25%, CI:4–48%) ($p < 0.022$) (Tables 2 and 3). When the percentage of sites with functional PDL regeneration is considered, the Ts/B (27%, CI:9–59%), H/B (25%, CI:8–55%), and R/B (25%, CI:8–55%) groups presented significantly higher values compared to EMD and Control, groups which did not present any sample with functional PDL regeneration (0%, CI:0–0%) ($p < 0.046$) (Tables 2 and 3).

Regarding the linear measurement of PDL regeneration within bone and tooth walls, no significant differences were detected between groups ($p > 0.10$), except for Ts/B and

TABLE 2. PERCENT EPITHELIAL TISSUE MIGRATION, MINERALIZED CEMENTUM, CEMENTUM AND CEMENTOID TISSUE, AND PERIODONTAL LIGAMENT REGENERATION CROSS TABULATION

	% Epithelial tissue migration		*% Mineralized cementum*		*% Mineralized cementum + cementoid*		*% PDL*		*% Functional PDL*	
Group	*No apical migration*	*Apical migration*	*Nonfull*	*Full*	*Nonfull*	*Full*	*Nonfull*	*Full*	*Nonfull*	*Full*
EMD	25.0%	75.0%	100.0%	0.0%	22.2%	77.8%	55.6%	44.4%	100%	0%
H/B	50.0%	50.0%	75.0%	25.0%	58.3%	41.7%	83.3%	16.7%	75%	25%
R/B	25.0%	75.0%	75.0%	25.0%	33.3%	66.7%	66.7%	33.3%	75%	25%
Control	10.0%	90.0%	100.0%	0.0%	60.0%	40.0%	90.0%	10.0%	100%	0%
Tp/B	40.0%	60.0%	90.9%	9.1%	36.4%	63.6%	72.7%	27.3%	90.9%	9.1%
Ts/B	10.0%	90.0%	72.7%	27.3%	27.3%	72.7%	36.4%	63.6%	72.7%	27.3%

Table 3. Estimated Marginal Means Percentage and Correspondent 95% Confidence Interval for Epithelial Tissue Migration, Mineralized Cementum, Cementum and Cementoid Tissue, and Full Periodontal Ligament Regeneration

	% Epithelial tissue migration		*% Mineralized cementum*		*% Cementum + Cementoid*		*% Full PDL*		*% Full functional PDL*	
Group	*Mean*	*95% wald CI*	*Mean*	*95% wald CI*	*Mean*	*95% wald CI*	*Mean*	*95% wald CI*	*Mean*	*95% wald CI*
EMD	75% AB	(38–94)%	0% B	(0–0)%	78% A	(42–94)%	44% A,B	(18–75)%	0% B	(0–0)%
H/B	50% A	(24–76)%	25% A	(8–55)%	42% A,B	(18–69)%	25% C	(4–48)%	25% A	(8–55)%
R/B	75% AB	(45–92)%	25% A	(8–55)%	67% A,B	(38–87)%	33% A,B,C	(13–62)%	25% A	(8–55)%
Control	90% B	(53–99)%	0% B	(0–0)%	40% B	(16–70)%	10% C	(1–47)%	0% B	(0–0)%
Tp/B	60% AB	(30–84)%	9% A,B	(1–44)%	63% A,B	(34–86)%	29% B,C	(9–59)%	9% A,B	(1–44)%
Ts/B	90% B	(53–99)%	27% A	(9–59)%	73% A,B	(41–91)%	62% A	(34–86)%	27% A	(9–59)%

Identical letters indicate statistically homogeneous groups.

Tp/B, where Ts/B (75%, CI: ±10.9%) demonstrated significantly higher mean values relative to Tp/B (38%, CI: ±23%) ($p<0.021$) (Fig. 7a). The other material combinations presented around 50% of full PDL regeneration. Although higher percentage of functional PDL for Ts/B (51%, CI: ±23%), EMD (47%, CI: ±25%), and H/B (49%, CI: ±22%) groups was detected, all group comparisons were statistically homogeneous (Fig. 7b).

Bone regeneration

In a temporal perspective, CT 3D reconstructions showed gradual BV increase for all groups along with defect filling and partial volumetric regeneration. At 2 weeks, EMD, H/B, Tp/B, and Ts/B groups presented no statistically significant difference relative to any other experimental group ($p>0.05$). The Control group (7.6%, CI: ±4.5%) presented the highest mean bone formation and R/B group (1.2%, CI: ±4.5%) the lowest estimated mean (significantly different between each other, $p<0.05$) (Fig. 8a). The group EMD (6.6%, CI: ±4.5%) presented significantly lower percentage of new bone relative to other groups at 4 weeks ($p=0.018$), except R/B (11.2%, CI: ±4.5%) ($p=0.163$) (Fig. 8b). At 6 and 8 weeks *in vivo*, statistical analysis depicted the lowest bone regeneration values for EMD group (12% and 12.9%, CI: ±4.5%, respectively) compared to others ($p<0.04$). Furthermore, Control, Tp/B, and Ts/B groups presented the highest mean percent bone formation (nonsignificant between each other), with Ts/B values significantly higher than EMD, H/B, and R/B ($p<0.025$). H/B and R/B groups presented intermediate estimated means with no statistically significant difference between each other (Fig. 8c, d).

Survey μCT 3D reconstruction and image thresholding of defects also depicted bone formation for all experimental groups with partial volumetric bone regeneration after 8 weeks *in vivo*. Regarding experimental group effect on percent bone formation, group EMD (13%, CI: ±4.5%) demonstrated the lowest estimated mean relative to others ($p=0.047$), except for R/B (19%, CI: ±4.5%). No significant difference was observed between Tp/B (31%, CI: ±4.5%), Ts/B (29%, CI: ±4.5%), R/B, H/B (21%, CI: ±4.5%), and Control (28%, CI: ±4.5%) groups ($p<0.05$) (Fig. 8e).

In agreement with the 3D reconstruction quantification, the histometric evaluation of bone formation within defect showed that Control (56%, CI: ±8.9%), Ts/B (53%, CI: ±8.9%), Tp/B (50%, CI: ±8.9%), and H/B (49%, CI: ±8.9%) groups presented the highest mean percentage (not significantly different between each other) followed by R/B (19%, CI: ±8.9%) and EMD (13%, CI: ±8.9%) groups. While the R/B mean values were significantly lower than Control

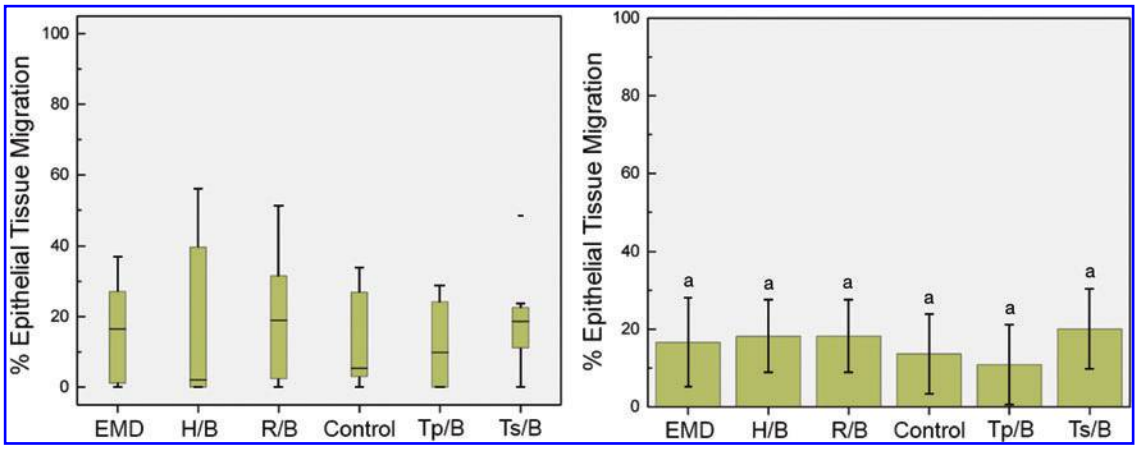

FIG. 5. Box plot and mean percentage ±95% confidence interval of epithelial tissue apical migration. *Identical letters* indicate statistically homogeneous groups. Color images are available online.

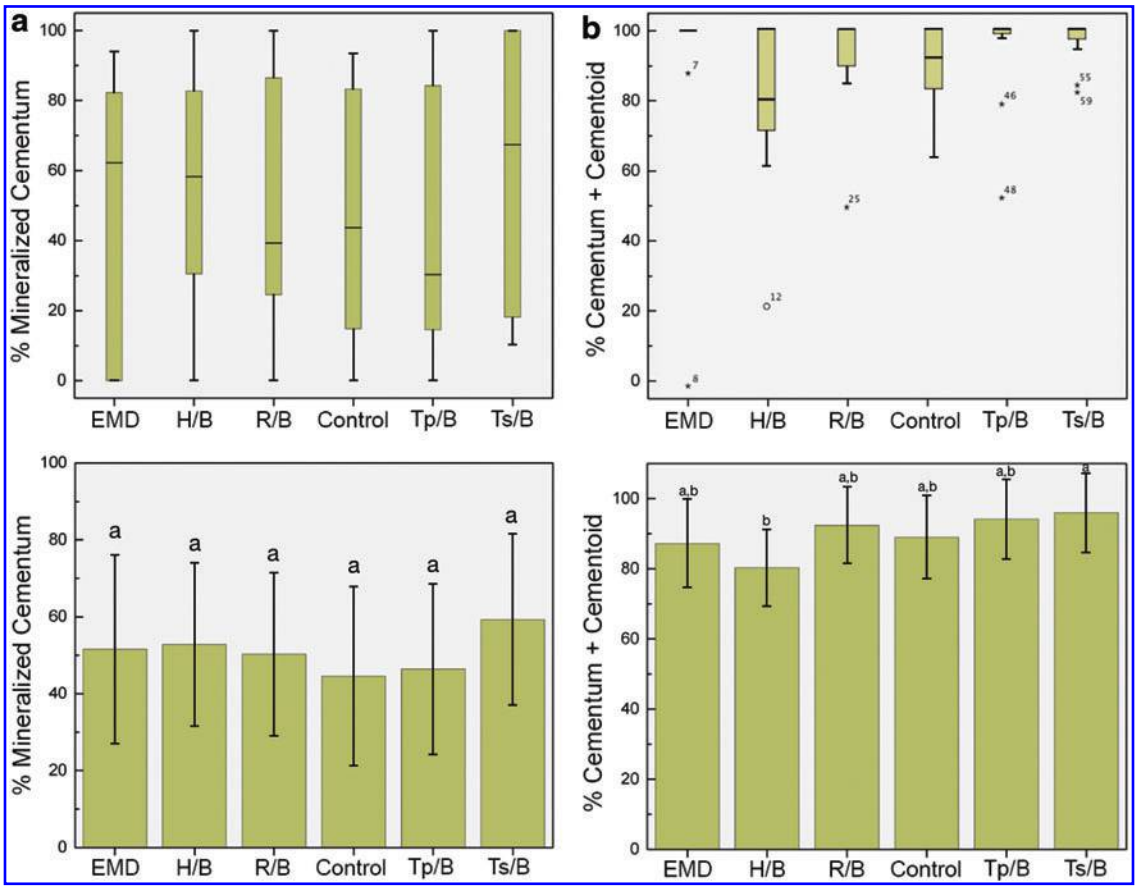

FIG. 6. *Box plot* and mean percentage ±95% confidence interval of **(a)** mineralized cementum and **(b)** cementum + cementoid tissue. *Identical letters* indicate statistically homogeneous groups. *Different letters* indicate statistically different groups. Color images are available online.

group ($p < 0.05$), EMD group presented significantly lower percentage of new bone relative to Control and Ts/B groups ($p < 0.02$) (Fig. 8f). The 2D analysis of the micrographs indicated no noticeable difference in the bone healing characteristics among groups. No considerable inflammatory cell remnants were observed for any experimental group. Histomorphology after 8 weeks *in vivo* demonstrated partial alveolar bone regeneration relative to original defect dimensions for all groups. Such newly formed bone, distinct from the pristine alveolar bone, was predominantly woven bone (Fig. 9). Ankylosis was not observed in any defect.

Discussion

The early stage of functional periodontal tissue regeneration essentially comprises the proliferation and the migration of PDL cells along the tooth root.[21] Nonetheless, the fastest migration rate of epithelial cells may impair the regeneration of cementum and PDL since they can first populate the root surface forming the long junctional epithelium.[6,7,31] The current gold standard procedure for preventing the downgrowth of the epithelium on the tooth-root surface encompasses the placement of physical barriers, as in the present study where it was placed in collagen sponges.[32] Such barriers are speculated to offer stability for the coagulum and, hence, avoid volume reductions and surface invaginations that otherwise will occur when the wound contracts.[31] In the current study, quantitative data showed no significant difference regarding EM with all groups presenting approximately 1 mm apical attachment relative to CEJ (~15% of defect depth), which is similar to the values obtained from previous studies using different growth factors and/or carriers.[12] The absence of significant difference between groups may be associated with the chemical agents used for debridement and dentin demineralization that remove the surface smear layer and expose organic components such as collagen matrix and promote the attachment of periodontal fibroblasts and suppress the epithelial tissue downgrowth.[32,33] In addition, matrix and growth factors, such as Emdogain and BDNF, have been shown to modulate the rate of cementum and PDL tissue formation, which contribute to the inhibition of epithelial cells to populate the root dentin and to accelerate the regeneration of a functional periodontal tissue.[11,34]

Cementum comprises the mineralized tissue that forms the outer surface of the tooth root and its development is crucial for functional periodontal tissue regeneration, which is structured with the newly formed cementum, alveolar bone, and connective tissue fibers functionally inserted into these hard tissues.[8] The results of the current study demonstrated promising outcomes in terms of regeneration when BDNF is locally delivered by collagen sponges. Although

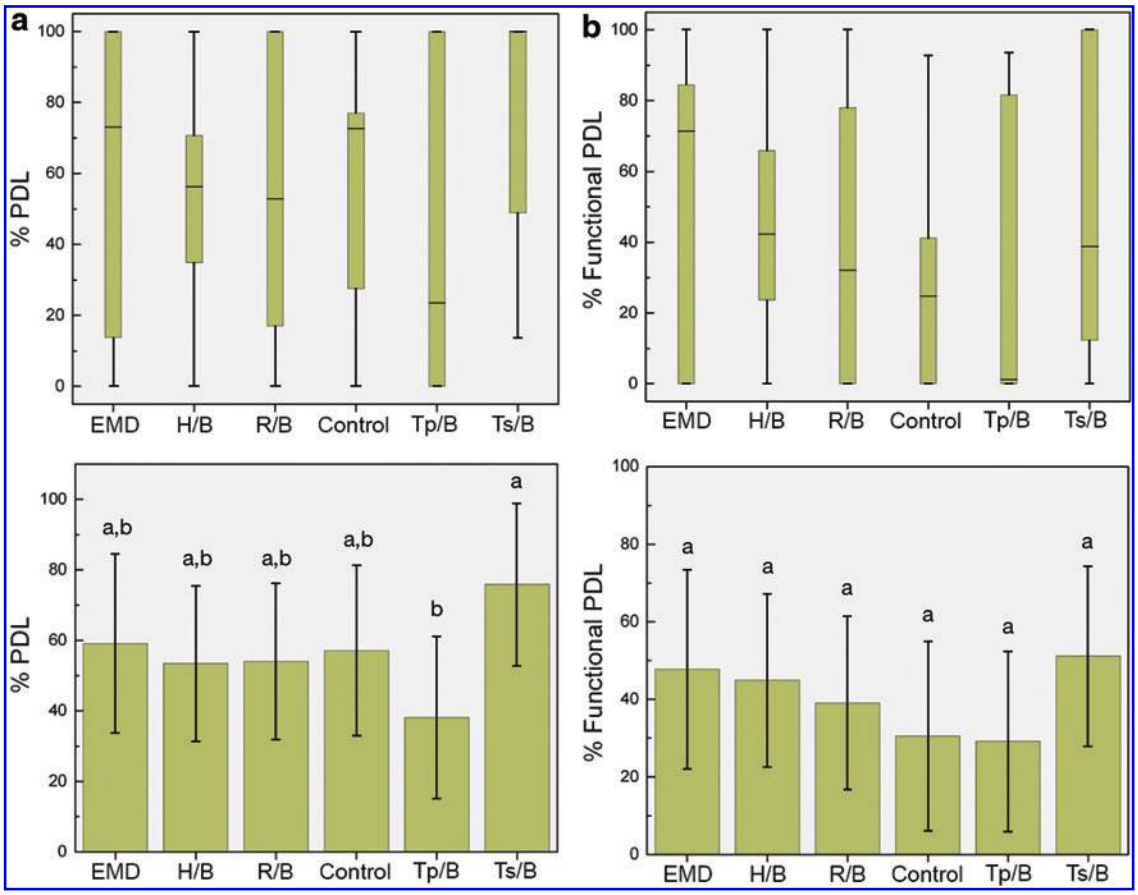

FIG. 7. Box plot and mean percentage ±95% confidence interval of **(a)** full PDL and **(b)** functional PDL within tooth and bone walls. *Identical letters* indicate statistically homogeneous groups. *Different letters* indicate statistically different groups. Color images are available online.

linear measurements did not demonstrate statistically significant difference between groups (approximately 50% of mineralized cementum regeneration), Ts/B, R/B, and H/B groups presented significantly higher percentage of samples (>25%) with mineralized cementum relative to EMS and Control (control groups), which did not present any sample with full-mineralized cementum regeneration (0%). In addition, the percentage of samples that presented mineralized cementum + cementoid tissue covering the root surface for Ts/B, R/B, and EMD groups represented more than 67% of the total number of samples (which is clinically relevant compared to 40% of samples for Control group). All the abovementioned evidence strongly suggests that Ts/B and R/B groups may have the potential to accelerate cementum regeneration (given that the EMD group presented high percentage of precementum, however, 0% samples converted to mineralized cementum after 8-week healing). Previous studies have also demonstrated the positive effect of BDNF on enhancing cementum regeneration using the same concentration of the current study, however, delivered by a different carrier (high-molecular weight–hyaluronic acid, HMW-HA).[10] While BDNF group presented 85% of samples with mineralized cementum regeneration, the negative control group demonstrated only 14% of samples with full regeneration.[10] The lower percentage of samples with full regeneration in the current study may be accounted for the differences in the defect model, which is a far more aggressive, one-wall critical defect, compared to the previously designed Class II furcation.

In terms of PDL regeneration, the regenerative potential of BDNF locally delivered by a collagen sponge can be again highlighted since higher percentage of samples with full PDL and functional PDL regeneration was demonstrated, mainly for Ts/B group. While in most instances no significant differences were detected in linear measurements (quantitative analyses) when one considers the full regeneration success of functional PDL after 8 weeks *in vivo* (statistically significant from EMD and Control) along with higher PDL formation and significantly high bone regeneration, it strongly suggests that regeneration takes place for Ts/B group in higher overall amounts and faster (by significantly higher mineralized cementum formation and conversion of 100% of these into functional PDL). Such results are clinically relevant since no full mineralized cementum and functional PDL were naturally regenerated (Control group). Interestingly, fourfold more samples with PDL regeneration for BDNF treated sites relative to a negative control group have been previously demonstrated corroborating with the current study trend in which BDNF stimulated PDL regeneration.[5]

Irrespective of the quantification method (3D or 2D), groups Control, Ts/B, Tp/B, and H/B presented the highest mean percentage of new bone formation (not significantly different between each other) followed by R/B and EMD

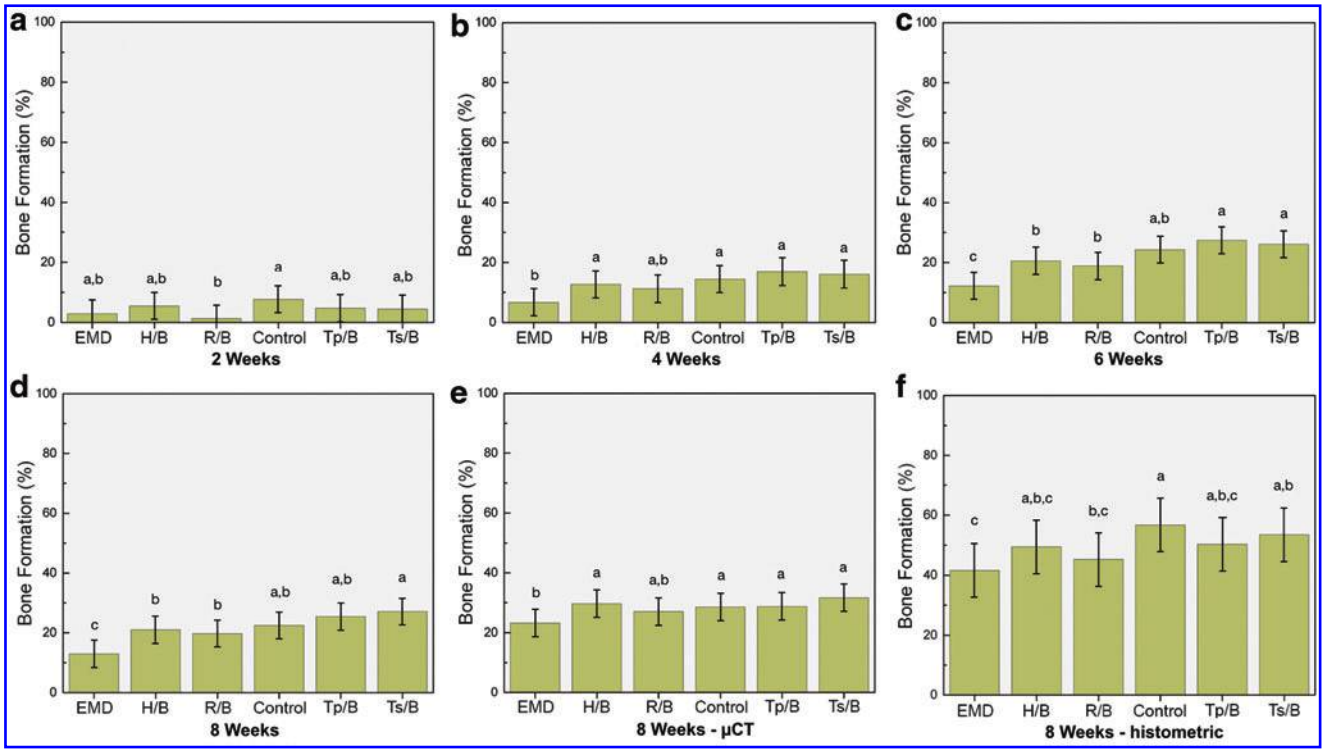

FIG. 8. Mean percentage ±95% confidence interval of bone formation within defect quantified through CT reconstructions at **(a)** 2-, **(b)** 4-, **(c)** 6-, and **(d)** 8 weeks *in vivo.* Percent bone formation within defect obtained using microCT **(e)** and 2D histometric quantification **(f)**. *Identical letters* indicate statistically homogeneous groups. *Different letters* indicate statistically different groups. Color images are available online.

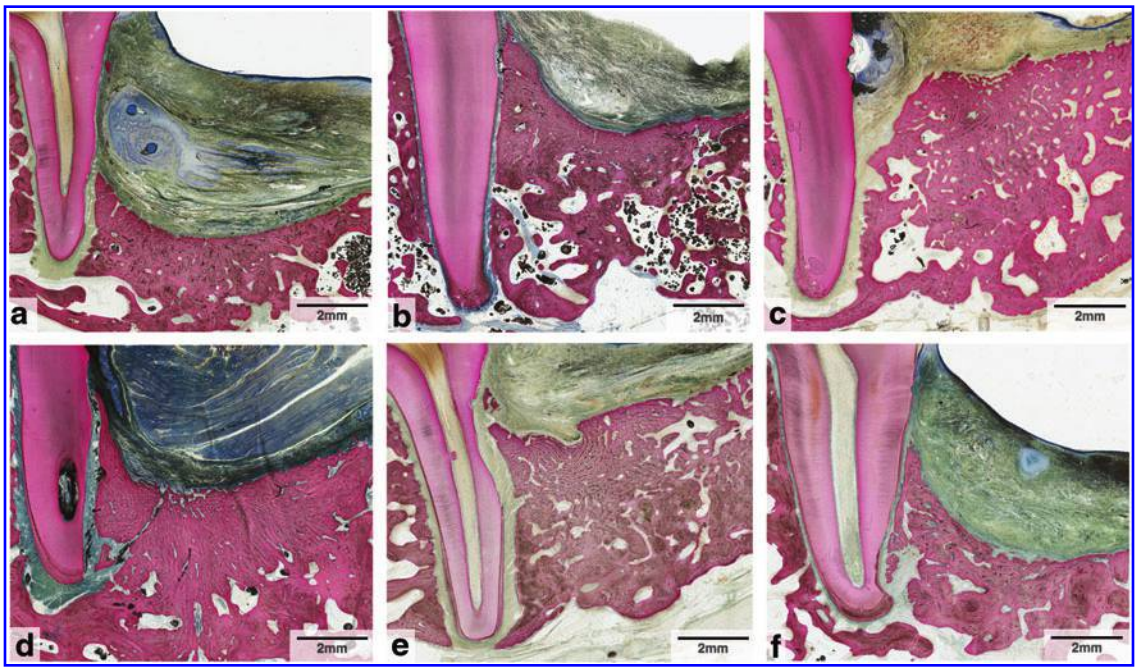

FIG. 9. Histologic sections of **(a)** EMD, **(b)** H/B, **(c)** R/B, **(d)** Control, **(e)** Tp/B, and **(f)** Ts/B groups after 8 weeks *in vivo*. The 2D analysis of the micrographs indicated no noticeable difference in the bone healing characteristics among groups. Histomorphology after 8 weeks *in vivo* demonstrated partial alveolar bone regeneration relative to original defect dimensions for all groups. Such newly formed bone, distinct from the pristine alveolar bone, was predominantly woven bone. EMD, enamel matrix protein derivatives. Color images are available online.

groups. Bone regeneration results significantly lower than most groups strongly suggest that the EMD group (Emdogain) may have functioned as a barrier for bone regeneration since the Control group (negative control) demonstrated significantly higher percentage of new bone formation. Concerning cementum and PDL regeneration, despite absence of significant difference in linear measurements relative to all BDNF/collagen combinations, EMD group primarily comprised no samples with full mineralized cementum and functional PDL regeneration (significantly lower than Ts/B, R/B, and H/B groups). While cementoid tissue allows for fiber insertion and PDL formation/organization, no EMD sample presented 100% mineralized cementum leading to functional PDL formation. Literature findings using similar methodology to analyze Emdogain regenerative capability also demonstrated equivalent levels of cementum and PDL regeneration relative to a negative control group and the use of collagen sponge alone.[14]

The current study design allowed also for the preliminary assessment of different collagen sponges as carriers for BDNF. The rationale for using a collagen plug was based on its favorable biological properties, such as hemostatic, chemotactic, and cell adhesive characteristics that stimulate cells to infiltrate, adhere, and synthesize new tissue.[25–29] In addition, it has been proven that collagen sponges also provide a continuous and sustained release of therapeutic agents over time.[35] In contrast, the main disadvantage of collagen-based scaffolds resides in their lack of rigidity. Previous studies have suggested that the structural integrity of collagen plugs is not ideal for critical defects, and they can readily become compressed due to soft tissue healing contraction producing less than desired BV regeneration.[36,37] Such assumption is supported by the results of the current study since all groups using collagen plug demonstrated similar percentage of bone regeneration relative to Control group (which theoretically presents the highest level of soft tissue contraction). A potential alternative in tissue engineering approaches comprises the use of particulate materials as carriers for growth factors. These materials have demonstrated improved compressive strength and a suitable environment for cell growth due to their favorable structural arrangement and osteoconductivity.[38] Previous literature findings have shown that hard scaffolds (as β-Tricalcium phosphate, β-TCP) resulted in enhanced periodontal tissue regeneration relative to collagen plugs, when loaded with a different growth factor.[12,13] Accordingly, studies addressing the use of hard particulate material carriers in combination with BDNF are warranted, where factor adsorption, release kinetics, and mechanical and degradation properties should be addressed in *in vitro* assays along with regeneration potential in preclinical *in vivo* studies.

Conclusion

Quantitative results for the tested formulations of BDNF carried by collagen sponges in a one-wall defect demonstrated that BDNF regenerates periodontal tissue to a level similar to control groups. Nonetheless, the combination of BDNF source and collagen sponge results in significantly more percentage of samples with full mineralized cementum for Ts/B, R/B, and H/B and functional periodontal ligament for Ts/B relative to control groups (EMD and Control). Thus, considering the combination of high bone formation along with higher full mineralized cementum and functional periodontal ligament, Ts/B combination is the most desirable for periodontal tissue regeneration of challenging defects.

Acknowledgments

The authors would like to thank the Dentsply Sirona (PI-PGC), for providing the funding to conduct this study, the Coordenação de Aperfeiçoamento de Pessoal de Nível Superior - Brasil (CAPES) - Finance Code 001 (grant no. 88881.132824/2016-0 and 88881.132654/2016-01) and the São Paulo Research Foundation (FAPESP)(grant no. 2016/17793-1; 2017/19362-0), for providing scholarships to I.R., E.B. and A.L.

Disclosure Statement

No competing financial interests exist.

References

1. Petersen, P.E., and Ogawa, H. Strengthening the prevention of periodontal disease: the WHO approach. J Periodontol **76,** 2187, 2005.
2. Tonetti, M.S., Jepsen, S., Jin, L., and Otomo-Corgel, J. Impact of the global burden of periodontal diseases on health, nutrition and wellbeing of mankind: a call for global action. J Clin Periodontol **44,** 456, 2017.
3. Barrington, E.P., and Nevins, M. Diagnosing periodontal diseases. J Am Dent Assoc **121,** 460, 1990.
4. Lindhe, J., Westfelt, E., Nyman, S., Socransky, S.S., Heijl, L., and Bratthall, G. Healing following surgical/non-surgical treatment of periodontal disease. A clinical study. J Clin Periodontol **9,** 115, 1982.
5. Jimbo, R., Singer, J., Tovar, N., *et al.* Regeneration of the cementum and periodontal ligament using local BDNF delivery in class II furcation defects. J Biomed Mater Res **106,** 1611, 2018.
6. Takeda, K., Shiba, H., Mizuno, N., *et al.* Brain-derived neurotrophic factor enhances periodontal tissue regeneration. Tissue Eng **11,** 1618, 2005.
7. Bosshardt, D.D., and Sculean, A. Does periodontal tissue regeneration really work? Periodontol 2000 **51,** 208, 2009.
8. Caton, J.G., and Greenstein, G. Factors related to periodontal regeneration. Periodontol 2000 **1,** 9, 1993.
9. Nohutcu, R.M., McCauley, L.K., Koh, A.J., and Somerman, M.J. Expression of extracellular matrix proteins in human periodontal ligament cells during mineralization in vitro. J Periodontol **68,** 320, 1997.
10. Jimbo, R., Tovar, N., Janal, M.N., *et al.* The effect of brain-derived neurotrophic factor on periodontal furcation defects. PLoS One **9,** e84845, 2014.
11. Kim, T.G., Wikesjö, U.M.E., Cho, K.S., *et al.* Periodontal wound healing/regeneration following implantation of recombinant human growth/differentiation factor-5 (rhGDF-5) in an absorbable collagen sponge carrier into one-wall intrabony defects in dogs: a dose-range study. J Clin Periodontol **36,** 589, 2009.
12. Kim, Y.T., Wikesjö, U.M.E., Jung, U.W., Lee, J.S., Kim, T.G., and Kim, C.K. Comparison between a beta-tricalcium phosphate and an absorbable collagen sponge carrier technology for rhGDF-5-stimulated periodontal wound healing/regeneration. J Periodontol **84,** 812, 2013.

13. Lee, J.S., Wikesjö, U.M.E., Park, J.C., *et al.* Maturation of periodontal tissues following implantation of rhGDF-5/beta-TCP in one-wall intra-bony defects in dogs: 24-week histological observations. J Clin Periodontol **39,** 466, 2012.
14. Shirakata, Y., Miron, R.J., Shinohara, Y., *et al.* Healing of two-wall intra-bony defects treated with a novel EMD-liquid-A pre-clinical study in monkeys. J Clin Periodontol **44,** 1264, 2017.
15. Wikesjo, U.M.E., Sorensen, R.G., Kinoshita, A., Jian Li, X., and Wozney, J.M. Periodontal repair in dogs: effect of recombinant human bone morphogenetic protein-12 (rhBMP-12) on regeneration of alveolar bone and periodontal attachment. A pilot study. J Clin Periodontol **31,** 662, 2004.
16. Barbacid, M. The Trk family of neurotrophin receptors. J Neurobiol **25,** 1386, 1994.
17. Ebendal, T. Function and evolution in the NGF family and its receptors. J Neurosci Res **32,** 461, 1992.
18. Kajiya, M., Shiba, H., Fujita, T., *et al.* Brain-derived neurotrophic factor stimulates bone/cementum-related protein gene expression in cementoblasts. J Biol Chem **283,** 16259, 2008.
19. Nosrat, I., Seiger, Å, Olson, L., and Nosrat, C.A. Expression patterns of neurotrophic factor mRNAs in developing human teeth. Cell Tissue Res **310,** 177, 2002.
20. Nosrat, C.A., Fried, K., Ebendal, T., and Olson, L. NGF, BDNF, NT3, NT4 and GDNF in tooth development. Eur J Oral Sci **106 (Suppl. 1),** 94, 1998.
21. Konishi, A., Takeda, K., Fujita, T., *et al.* Sequential process in brain-derived neurotrophic factor-induced functional periodontal tissue regeneration. Eur J Oral Sci **124,** 141, 2016.
22. Nakanishi, T., Takahashi, K., Aoki, C., Nishikawa, K., Hattori, T., and Taniguchi, S. Expression of nerve growth factor family neurotrophins in a mouse osteoblastic cell line. Biochem Biophys Res Commun **198,** 891, 1994.
23. Stähli, A., Miron, R.J., Bosshardt, D.D., Sculean, A., and Gruber, R. Collagen Membranes Adsorb the Transforming Growth Factor-beta Receptor I Kinase-Dependent Activity of Enamel Matrix Derivative. J Periodontol **87,** 583, 2016.
24. Susin, C., Fiorini, T., Lee, J., De Stefano, J.A., Dickinson, D.P., and Wikesjö, U.M.E. Wound healing following surgical and regenerative periodontal therapy. Periodontol 2000 **68,** 83, 2015.
25. Locci, P., Becchetti, E., Pugliese, M., *et al.* Phenotype expression of human bone cells cultured on implant substrates. Cell Biochem Funct **15,** 163, 1997.
26. Postlethwaite, A.E., Seyer, J.M., and Kang, A.H. Chemotactic attraction of human fibroblasts to type I, II, and III collagens and collagen-derived peptides. Proc Natl Acad Sci U S A **75,** 871, 1978.
27. Yaffe, A., Ehrlich, J., and Shoshan, S. Restoration of periodontal attachment employing enriched collagen solution in the dog. J Periodontol **55,** 623, 1984.
28. Bunyaratavej, P., and Wang, H.L. Collagen membranes: a review. J Periodontol **72,** 215, 2001.
29. Behring, J., Junker, R., Walboomers, X.F., Chessnut, B., and Jansen, J.A. Toward guided tissue and bone regeneration: morphology, attachment, proliferation, and migration of cells cultured on collagen barrier membranes. A systematic review. Odontology **96,** 1, 2008.
30. Takeda, K., Sakai, N., Shiba, H., *et al.* Characteristics of high-molecular-weight hyaluronic acid as a brain-derived neurotrophic factor scaffold in periodontal tissue regeneration. Tissue Eng Part A **17,** 955, 2011.
31. Cardaropoli, G., Araujo, M., Hayacibara, R., Sukekava, F., and Lindhe, J. Healing of extraction sockets and surgically produced - augmented and non-augmented - defects in the alveolar ridge. An experimental study in the dog. J Clin Periodontol **32,** 435, 2005.
32. Kosen, Y., Miyaji, H., Kato, A., Sugaya, T., and Kawanami, M. Application of collagen hydrogel/sponge scaffold facilitates periodontal wound healing in class II furcation defects in beagle dogs. J Periodont Res **47,** 626, 2012.
33. Blomlof, J., Blomlof, L., and Lindskog, S. Effect of different concentrations of EDTA on smear removal and collagen exposure in periodontitis-affected root surfaces. J Clin Periodontol **24,** 534, 1997.
34. Miron, R.J., D. Bosshardt, D.D., Hedbom, E., *et al.* Adsorption of enamel matrix proteins to a bovine-derived bone grafting material and its regulation of cell adhesion, proliferation, and differentiation. J Periodontol **83,** 936, 2012.
35. Huang, F., Yin, Z., Wu, D., and Hao, J. Effects of controlled release of brain-derived neurotrophic factor from collagen gel on rat neural stem cells. Neuroreport **24,** 101, 2013.
36. Fiorellini, J.P., Howell, T.H., Cochran, D., *et al.* Randomized study evaluating recombinant human bone morphogenetic protein-2 for extraction socket augmentation. J Periodontol **76,** 605, 2005.
37. Tatakis, D.N., Koh, A., Jin, L., Wozney, J.M., Rohrer, M.D., and Wikesjo, U.M.E. Peri-implant bone regeneration using recombinant human bone morphogenetic protein-2 in a canine model: a dose–response study. J Periodont Res **37,** 93, 2002.
38. Inzana, J.A., Olvera, D., Fuller, S.M., *et al.* 3D printing of composite calcium phosphate and collagen scaffolds for bone regeneration. Biomaterials **35,** 4026, 2014.

Address correspondence to:
Ilana Ramalho, DDS, MSc
Department of Prosthodontics and Periodontology
Bauru School of Dentistry
University of Sao Paulo
Alameda Octávio Pinheiro Brisola 9-75
Bauru 17012-901
Brazil

E-mail: ilanaramalho@hotmail.com

Received: July 25, 2018
Accepted: November 7, 2018
Online Publication Date: January 18, 2019